Synthesis and Characterization of Amine-Functionalized Mixed-Ligand Metal-Organic Frameworks of UiO-66 Topology

S. M. Chavan,G. C. Shearer,S. Svelle,U. Olsbye,F. Bonino,J. Ethiraj,K. P. Lillerud,S. Bordiga
Synthesis and Characterization of Amine-Functionalized Mixed-Ligand Metal-Organic Frameworks of UiO-66 Topology
INORGANIC CHEMISTRY (2014) 53
DOI: 10.1021/ic500607a

Synthesis and Characterization of Amine Functionalized Mixed Ligand Metal-organic Frameworks of UiO-66 topology

Sachin M. Chavan[a*], Greig C. Shearer[a], Stian Svelle[a], Unni Olsbye[a], Francesca Bonino[b], Jayashree Ethiraj[b], Karl Petter Lillerud[a] and Silvia Bordiga[a,b*]

[a]*inGAP Center of Research Based Innovation, Department of Chemistry, University of Oslo, P.O. Box 1033, Blindern, 0315 Oslo, Norway*

[b]*Department of Chemistry, NIS and INSTM Reference Centre, University of Turin, Via G. Quarello 15 I-10135 Torino, Italy*

Abstract: A series of amine functionalized mixed linker–MOFs of idealized structural formula $Zr_6O_4(OH)_4(BDC)_{6-6X}(ABDC)6_X$ (BDC = benzene-1,4-dicarboxylic acid, ABDC = 2-aminobenzene-1,4-dicarboxylic acid) has been prepared by solvo- thermal synthesis. The materials have been characterized by TGA, PXRD and FTIR spectroscopy with the aim of elucidating the effect that varying degrees of amine functionalisation has on the stability (thermal and chemical) and porosity of the framework. This work includes the first application of UV-visible spectroscopy in the quantification of ABDC in mixed linker–MOFs.

1. Introduction

Metal-organic frameworks are crystalline materials that comprise metal ions or clusters coordinated to often rigid organic molecules forming three- dimensional porous structures.[1-4] This combination of inorganic and organic building blocks gives rise to near infinite structural and chemical possibilities. Such potential has resulted in these materials generating great interest in gas separation/storage,[5-6] catalysis,[7-9] and drug delivery[10-11] applications. One emerging area which opens yet more possibilities is Post-Synthetic Modification (PSM).[12-13] To this end, the basicity and reactivity of pendant -NH_2 groups has resulted in amine functionalized MOFs being the most often exploited materials for this purpose.[14-17] Moreover, many amine functionalized MOFs have shown improved CO_2 uptake[18-20] versus their non-functionalized, isostructural analogues. Designing MOFs with tailored functional sites is the path way to develop materials for advanced applications. However, often it has been found that fully functionalized materials are thermally less stable; imposing challenges in solvent removal and activation of the framework.[15, 21] In order to circumvent this problem, it has recently been shown that diluting the extent of functionalisation via a "mixed linker" (ML) approach is effective tuning the stability of

the material.[22-25] Furthermore, varying the composition of mixed linker–MOFs can result in systematic alteration of the gas adsorption capacity and selectivity of the material. Such an approach has been previously been adopted on several MOF topologies, namely MOF-5,[26] MIL-53-Al,[27-28] CAU-10,[29] and MIL-101[30] where a mixture of benzene-1,4-dicarboxylic acid (BDC) and its amino-, bromo-, nitro-, methyl- functionalized derivatives were used as linkers. In these studies, various properties of the materials were significantly influenced by the amount and type of functionality introduced in to the framework; namely the surface area (MOF-5),[26] the breathing pressure (MIL-53)[28] and sorption properties (CAU-10)[29] were observed to have been affected. In order to design mixed linker–MOFs for a particular purpose, it is important to first gain an understanding of how the properties of the materials are affected by altering the ratio between the linkers. To allow such correlations to be made, mixed linker–MOFs with varying degrees of functionalization must be synthesized and thoroughly characterized.

UiO-66,[31-34] a Zr(IV)-based MOF has recently received great interest due to its high thermal and chemical stability. In accordance with observations on other framework types, UiO-66-NH_2, the fully amino functionalized isostructural analogue, is thermally less stable than unmodified UiO-66.[15] Moreover, post-synthetic modification of UiO-66-NH_2 can be challenging due to the steric hindrance imposed by the large density of pendant –NH_2 groups pointing into the cavities.[35-37] The desired –NH_2 content may thus vary depending on the application, i.e. it may be beneficial to maximize –NH_2 loading for the carbon capture and storage applications, whereas a more diluted –NH_2 loading might be preferred from a post-synthetic modification and catalysis point of view.

The only existing study on amine based mixed linker–MOFs of the UiO-66 topology was reported by Kim et al.[38] Where a mixture of amino- and bromo- functionalized BDC was used to form UiO-66-Br-NH_2, a MOF which was found to be more thermally stable than UiO-66-NH_2. Moreover, selective post-synthetic modification of these functional groups in mixed linker–MOF was demonstrated.

In this contribution, we present the synthesis and characterization of mixed linker–MOFs of the UiO-66 framework topology, prepared using a mixture of BDC and 2-aminobenzene-1,4-dicarboxylic acid (ABDC). The series of samples has been characterized for their thermal and chemical stability; ease of activation and porosity. Following the use of an original digestion

method (OH^- instead of F^- based media) the ABDC content of the MOFs was quantified by UV-visible spectroscopy for the first time, with the results validated by the more conventional ^1H NMR method.

2. Materials and Methods

2.1 Material Synthesis All chemicals were obtained from commercial vendors and used without further purification. The reaction mixtures were prepared in a volumetric flask by sequentially adding N,N-dimethylformamide, $ZrCl_4$, H_2O, and linker, and in a 350 : 1 : 1.3 : 1 molar ratio at room temperature. The linker portion consisted of five different mixtures of BDC and ABDC, resulting in five different materials. Specifically, the molar fractions of ABDC with respect to BDC were: 0, 0.25, 0.50, 0.75, and 1. The five resulting materials are hereafter labeled UiO-66, UiO-66-NH_2-25, UiO-66-NH_2-50, UiO-66-NH_2-75, and UiO-66-NH_2, respectively. See Table S1 for the masses of the synthesis reagents. The flasks were then sealed and placed in an oven at 100 °C where the synthesis was performed under static conditions for 72 hours. The resulting products precipitated as microcrystalline powders which were then separated from the solution by centrifugation and washed three times in DMF (40 mL). Water exchanged samples were obtained by washing the materials three times in excess of water at 80 °C for 2 hours. Finally, all the samples were dried at 60 °C in air for 24 hours. All syntheses were successfully reproduced and resulted in a 90-95 % yield of MOF material. In a parallel study by our group, the UiO-66 synthesis conditions have been optimized in order to limit the number of missing linkers. A second set of mixed ligand BDC/ABDC UiO-66 samples has been synthesized based on this method and is described in section F of the supporting information.

2.2Methods

2.2.1Physico-chemical characterization Powder X-ray diffraction patterns were collected on a Bruker D8 Discovery diffractometer equipped with a focusing Ge-monochromator, using Cu-K_α radiation(xx=1.5418 Å) and a Bruker LYNXEYE detector. PXRD were collected in reflectance Bragg-Brentano geometry in the 2θ range from 3 to 50°. Thermo-gravimetric analysis was performed on typically ca. 25-30 mg of powdered sample loaded inside a platinum crucible on a Stanton Redcroft TG-DSC instrument. Samples were heated at a ramp 5 $^\circ$C per minute to 700 $^\circ$C; under the flow of N_2 and O_2 with flow rates 20 and 5 mL per minute respectively. Nitrogen sorption measurements were performed on a BelSorb mini II instrument at 77 K. Prior to

adsorption measurements samples were pretreated (activated) under vacuum for 1h at 80 °C and 2 h at 200 °C. Brunauer–Emmett–Teller (BET) and Langmuir surface areas were calculated by fitting the isotherm data in the p/p_0 range of 0 - 0.1. The chemical stability of the MOFs was evaluated by suspending the samples in water (RT for 1 month, 100 °C for 24 h), 1M HCl (24h) and 1M NaOH (24h) in separate experiments. To confirm the framework stability, powder XRDs were measured before and after the chemical treatment for each sample.

2.2.2 Quantitative analysis of linker Prior to measurement, MOF samples were digested by adding a weighed amount of sample (10-20 mg for UV-vis, 20 mg for ^{1}H NMR) to a 1M NaOH-H_2O solution (for Uv-vis) and 600 μL of a 1M NaOH-D_2O solution (for ^{1}HNMR) and allowing the mixture to stand for 24 Hours. This hydroxide based procedure dissolves only the organic portion of the material (linker and pore filling solvent), while the inorganic component of the MOF form zirconium hydroxide, which sinks to the bottom and is not measured. Both absorbance and reflectance, UV-visible spectra were collected on a Shimadzu UV-3600 spectrophotometer. The spectra were recorded in 200-800 nm wavelength range. ^{1}H NMR spectra were recorded on Bruker Avance DPX-300 NMR Spectrometer (300 MHz). The relaxation delay (d1) was set to 20 seconds to ensure that reliable integrals were obtained, allowing for the relative concentrations of the various organic species to be accurately determined. The number of scans was 64.

3 .Results and Discussion

3.1 Synthesis and Structure: The simplest way to prepare mixed linker–MOFs is to use a mixture of isostructural linkers of similar denticity and utilize them in a procedure closely resembling that used to obtain the non-functional analogue. Only few examples in the literature that follow such an approach, with most groups instead are optimizing the synthesis conditions specifically to obtain mixed linker–MOFs. Kleist et al[26] have reported that the choice of reaction conditions plays a crucial role in the synthesis of mixed linker–MOFs based on the MOF-5 structure. Lammert et al[30] also found that both the metal precursor and the solvent plays a key role in the synthesis of mixed linker–MOFs in MIL-101 system. In this work on the UiO-66 topology, mixed linker–MOFs and phase pure UiO-66 and UiO-66-NH_2 were successfully prepared under very similar synthesis conditions. The PXRD patterns of samples prepared with

25, 50, 75 mol% of ABDC are reported in Figure1, clearly showing the crystalline nature of all the samples and matches perfectly with patterns of phase pure UiO-66 and UiO-66-NH_2 confirming the synthesis of isostuctural mixed-linker frameworks with a FCC structure.

Refinements of the PXRD patterns using Pawley method (Accelyer Material studio 6.6) show no significant change in the lattice parameter, 20.77 to 22.74Å, going from UiO-66 to UiO-66-NH_2. This very small change in the lattice constant and small size of crystallites (SEM ~100nm) does not allow us to gather information on the distribution of linkers.

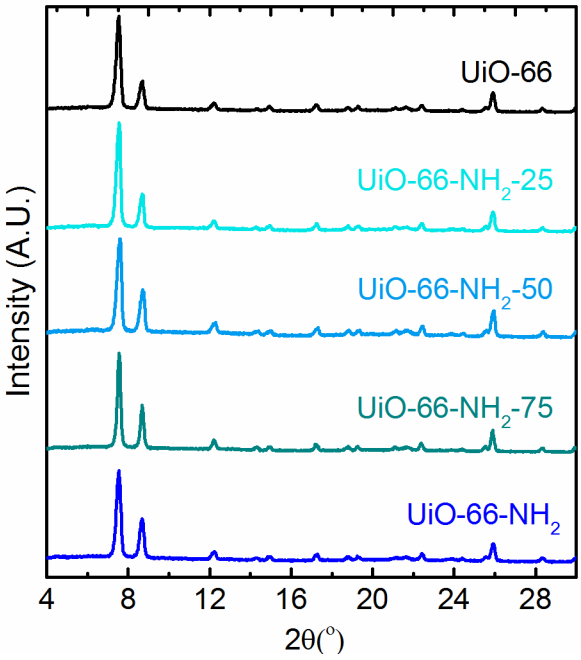

Figure 1. Comparison of the powder X-ray diffraction patterns of the mixed linker–MOF series. PXRD patterns up to 50°, 2θ are given in Figure S1.

3.2 Quantitative analysis of linkers

Quantitative analysis of linkers in MOFs (in particular ABDC) has been done by measuring the solutions obtained by disassembling the framework in an appropriate media. Although the disassembly of Zr-MOFs in 1M NaOH was reported[15] before the recent development of fluoride based media,[17] it had not been exploited further as a digestive media for quantitative analysis. The toxicity associated with fluoride based media and has led us to opt to continue working with 1M NaOH solution for MOF disassembly. Moreover, the analysis (PXRD and TGA-DSC, Figure

S4) of the undissolved solid obtained after the disassembly of MOF in 1M NaOH shows no sign of residual organic linker that confirms all the linker present at MOF is dissolved in solution.

DR-UV-Vis spectroscopy measurements (Figure S2, supporting information) provided a qualitative indication that the fraction of ABDC in the materials decreased in the order UiO-66-NH_2 > UiO-66-NH_2-75 > UiO-66-NH_2-50 > UiO-66-NH_2-25 as would be expected. This was evidenced by the decreasing intensity of a band at λ_{max} = 328 nm in the DR-UV-Vis spectra. This band is assigned to the electronic transition from the non-bonding to anti-bonding molecular orbital of ABDC (n→π*) and is responsible for the yellow color of both the linker molecule and the MOFs it forms.[34] In order to quantify the ABDC content with UV-visible spectroscopy, a calibration curve (inset of Figure 2) is required, allowing the Beer-Lambert law to be applied. The curve was obtained by recording the absorption spectra of standard solutions of ABDC of varying concentration in a 1M NaOH media. The spectral absorbance at 329 nm was then plotted against the concentration. The absorbance spectra of the standard solutions are given in the supporting information (Figure S3).

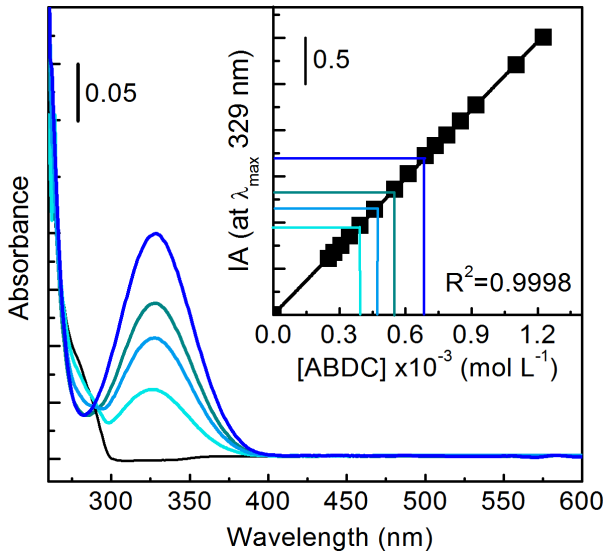

Figure 2. a) Uv-visible absorbance spectra of MOFs disassembled in 1M aqueous NaOH solution for 24h: UiO-66-NH_2, UiO-66-NH_2-75, UiO-66-NH_2-50, UiO-66-NH_2-25, and UiO-66. The inset shows the calibration curve obtained by plotting the integrated absorbance (IA) at λ_{max} 329nm of a standard solution of ABDC against concentration.

The concentration of ABDC in the MOFs can then be determined by measuring absorption spectra on the digest solutions and interpolating the absorbance at 328 nm on the calibration curve. Table S2 details the method used to calculate the ABDC content in the mixed linker–MOFs using this data.

Providing a qualitative illustration of the results, Figure 3 shows the normalized ^{1}HNMR spectra obtained on the digestion solutions of all five samples in the series. As expected from the UV-vis data, when going through the series from UiO-66 to UiO-66-NH_2, the ABDC proton signal (3 × 1H, part b) systematically increases in intensity while the BDC proton signal (4H, part a) decreases. This result confirms that, ABDC substitutes for BDC to an increasing extent throughout the series.

The quantitative analysis of these results (see section E of the supporting information for details of the method) affords the values presented in Table 1 alongside those of the UV-visible spectroscopy results. It can be seen that the values for ABDC content obtained by both spectroscopic methods are in satisfactory agreement. This validates the use of UV-Visible spectroscopy applied to the quantitative analysis of ABDC containing mixed linker–MOFs. Furthermore, it is seen that the extent to which the substituted linker is incorporated into the crystalline product is nearly the same as that expected by the ABDC:BDC ratio used in the synthesis mixtures. This was found not to be the case for another synthesis method where an excess of linker (2:1 ligand to metal ratio) was used. There, the results indicated a clear preference for the non-functionalised BDC linker (see section F of the supporting information for more details).

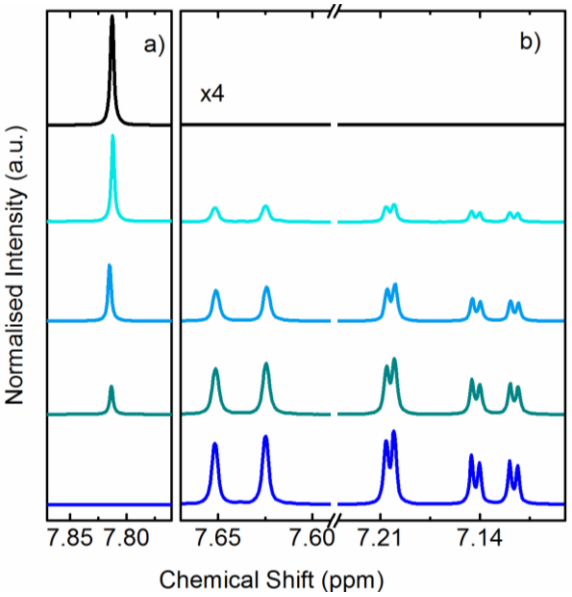

Figure 3. Normalized [1]HNMR spectra of the mixed linker–MOFs series digested for 24h in a 1M solution of NaOH in D_2O: UiO-66-NH_2, UiO-66-NH_2-75, UiO-66-NH_2-50, UiO-66-NH_2-25, and UiO-66. Proton signal associated with BDC (Part a) and Signals associated with ABDC (Part b). Signals in part b are multiplied by the factor of 4 for easy visual comparison of the signal intensities.

Table 1. mol % of ABDC used in the synthesis of mixed linker–MOFs are compared with mol% of ABDC determined by UV-visible and NMR spectroscopy.

MOF	[ABDC] mol %		
	Synthesis	UV-Vis	NMR
UiO-66	0	0	0
UiO-66-NH_2-25	25	30	30
UiO-66-NH_2-50	50	54	57
UiO-66-NH_2-75	75	70	77
UiO-66-NH_2	100	104	100

3.3 Thermal stability and activation

Activation, the process of solvent removal from the pores of the framework, allows access to the porosity to the sample and thus an important step in the development of MOFs for commercial applications as adsorbents and as catalysts.[21] Many MOFs are synthesized in DMF, which has a high boiling point and is strongly adsorbed inside the pores, especially so in MOFs with a high

loading of polar functional groups such as amines. The complete removal of such strongly adsorbed molecules usually requires high temperatures (ca. 250 ^{o}C) and the application of vacuum conditions which cause many MOFs to decompose. This problem can be overcome by post synthetically exchanging DMF with more volatile solvents which do not affect the crystallinity of the samples.[21] In this work, activation was facilitated by the post synthetic exchange of DMF with water, a procedure which proved to be very effective, especially in samples with high amino content. In order to investigate the effect that the ABDC content has on the thermal stability and activation of the frameworks, all five samples in the series were characterized by TGA, thermal treatments followed by PXRD, and FTIR spectroscopy.

3.3.1 Thermo-gravimetric Analysis

Figure 4a and 4b present the TG-DSC results of the as-synthesized and water exchanged samples respectively. Three steps weight loss are observed on the TGA curves of the as synthesized samples. The initial 5-6% weight loss is observed up to 80 °C, while the second (25-28%) is observed in the range 100-280 °C. Such weight losses are due to the removal of solvent and the dehydroxylation of the zirconium oxo-clusters. The third and last weight loss step is due to the framework decomposition (Tdec) and, occurs at a slightly different temperature on each

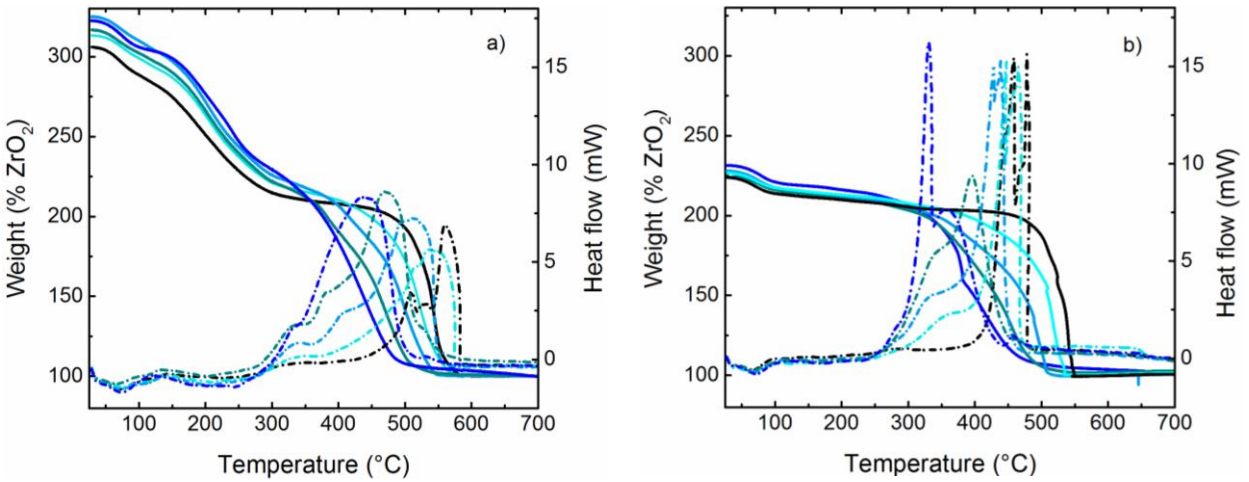

Figure 4. TG-DSC results of as prepared (part a) and water washed (part b) MOFs: UiO-66.; UiO-66-NH_2-25; UiO-66-NH_2-50; UiO-66-NH_2-75 and UiO-66-NH_2. TGA curves are reported in solid lines, while the DSC curves are dash-dotted. The end weight of the TGA run is normalized to 100% of ZrO_2, expected product in the aerobic thermal decomposition of Zr-MOF.

In case of UiO-66-NH_2, UiO-66-NH_2-75 and UiO-66-NH_2-50 this last step is not preceded by a clear plateau, indicating that the framework in fact starts to decompose before the solvent is totally removed. One last observation from the TGA curves is that there is a clear systematic increase in the decomposition temperature of the framework as the loading of ABDC in the framework decreases. A similar trend of stability has been observed in IRMOF-3/ MOF-5 based mixed ligand frameworks.[26] The DSC data reported in Figure 4a clearly indicates the exothermic nature of the framework decomposition, corresponding to the burning of linkers. In order to determine whether the mixed linker–MOF microcrystals studied in this work contain randomly distributed linker or are simply a physical mixture of pure UiO-66 and UiO-66-NH_2 MOFs phases, a separate TG-DSC experiment was performed on a physically mixed UiO-66 and UiO-66-NH_2 (molar ratio 1:1) sample. These results are compared to that obtained on the UiO-66-NH_2-50 sample in Figure S7. It is found that very little difference can be observed between the two samples on the basis of their TGA results however; the DSC curves of the two measurements have clearly distinct profiles. In particular, the DSC curve of the physical mixture shows two well separated heat signals at 430 (broad) and 490 $^{\circ}$C (sharp), corresponding to the decomposition of the UiO-66 and UiO-66-NH_2 phases respectively. In contrast, the decomposition to the decomposition of UiO-66-NH_2-50 sample is signified by only a single, broad peak extending over a temperature range of 400-50 $^{\circ}$C. This result provides convincing evidence that the linkers of the samples prepared here are indeed randomly distributed linker from crystal to crystal and are not just a physical mixture of the UiO-66 and UiO-66-NH_2 MOFs phases.

Figure 4b shows the TG-DSC results for the water exchanged samples. Each MOF sample loses 5-6 % of their initial weight in the temperature range 25-250 $^{\circ}$C, and is indicative of the removal of water from the pores. This weight loss is very small compared with the equivalent weight losses observed in the DMF containing as synthesized samples, suggesting that the DMF was removed very effectively by the water exchange procedure. Moreover, the solvent exchange seems to have had no effect on the decomposition temperature of the materials such that the previously established relation between the ABDC content and framework stability is maintained. The DSC curves of the water washed samples suggest that the decomposition of the framework is more sharply defined and exothermic when compared to the as synthesized

samples. This is likely due to the fact that the decomposition is no longer occurring simultaneously with the endothermic solvent removal process, allowing the observation of the framework collapse as a much more precise exothermic event.

3.3.2 Infrared spectroscopy

While TG-DSC profiles are very useful for following the behavior of samples during the heat treatments, and helping to identify suitable activation conditions, PXRD and FTIR are the techniques of choice for ensuring that the samples remain intact after the specific activation procedure. The full set of samples in the as synthesized and water washed forms as well as after thermal treatment at 200 $^{\circ}$C for 12 hours in air have been measured by both PXRD and DRIFT spectroscopy. The DRIFT results are displayed in Figure 5. Generally speaking it is possible to follow the solvent exchange and removal (progressive decreasing of specific finger print due to the solvent) and/or MOF framework decomposition (broadening of the bands below 1650 cm^{-1}. Other noteworthy observations from the DRIFT results are as follows: i) a strong absorption band at about 1665 cm^{-1} (dashed pink line), assigned to the ν(C=O) stretching of DMF, is seen only in the synthesized samples. The absence of this band in the water exchanged samples, gives additional evidence for the complete exchange of DMF with water;[32] ii) absorption bands at 1338 and 1261 cm^{-1} (dashed grey line, associated with ABDC) are seen to increase in intensity, as the ABDC content of the MOF increases; iii) the IR spectra collected after the thermal treatment show no broadening or weakening of the absorption bands, testifying that no dramatic change in the long range order of the material has taken place. This is backed up by the corresponding PXRD patterns shown in Figure S8 in the supporting information. The patterns show that all the samples retain high crystallinity even after a prolonged thermal treatment. To our knowledge, such rigorous thermal stability tests (12h treatment) have not been reported before on any MOF.

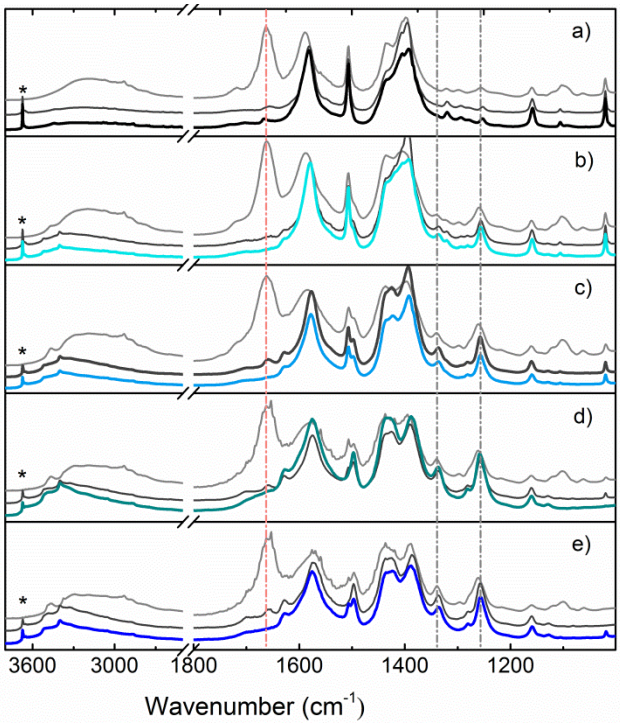

Figure 5. DRIFT spectra of a) UiO-66, b) UiO-66-NH_2-25, c) UiO-66-NH_2-50, d) UiO-66-NH_2-75 and e) UiO-66-NH_2. Three curves from top to bottom represent the sample as prepared (grey), water washed (dark grey) and after heating for 12h at 200 °C in air (same color code as in previous figures). DRIFT spectra were recorded on samples diluted with KBr. The pink and grey dash-dot lines mark the peaks associated with DMF and ABDC linker respectively, while the asterisks shows the absorption peak associated with hydroxyl groups on the Zr-clusters.

3.3.3 N_2 sorption

Nitrogen sorption isotherms measured at 77K on the samples which were exchanged for water are shown in Figure 6. All the samples were heated at 200 °C for 2 hours under vacuum prior to the adsorption of nitrogen.

All the samples show type-I isotherms, confirming the microporous nature of the mixed linker–MOFs. The fully functionalized amino MOF is less porous than the parent UiO-66. This is as expected since the NH_2 group will block some of the void space.[15] Moreover, the surface area and pore volume is observed to systematically decrease (inset Figure 6) as the ABDC content of the framework increases. Table 2 lists the surface area (BET and Langmuir) and pore volumes of the samples calculated using the data in the p/p_0 range 0 - 0.10 of the isotherm. All samples were found to remain intact after solvent removal, as evidenced by PXRD measurements performed on the materials following these N_2 adsorption measurements (Figure S9). While the addition of NH_2 functional groups reduces the internal volume, missing linkers

will have the opposite effect. The surface area for the parent UiO-66 indicates that 3 of 24 linkers are missing.[39] Changes in linker ratio in the synthesis will probably also alter the amount of missing linkers prohibiting a quantitative calculation of amine substitution based on absorption measurements alone.

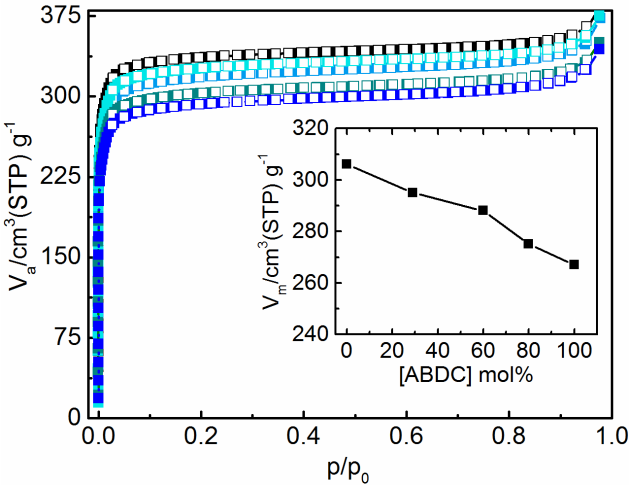

Figure 6. N_2 sorption isotherm at 77K measure on water washed samples of UiO-66; UiO-66-NH_2-25, UiO-66-NH_2-50, UiO-66-NH_2-75, and UiO-66-NH_2. The solid and open squares symbols represent the adsorption and desorption loop, respectively.

Table 2. Surface areas and pore volume (V_m) of MOFs calculated from the N_2 sorption isotherm at 77K. Prior to the N_2 adsorption both samples were pretreated under vacuum for 1h at 80 °C and for 2h at 150 °C.

Sample	BET [m^2 g^{-1}]	Langmuir [m^2 g^{-1}]	Vm [cm^3(STP) g^{-1}]
UiO-66	1331	1444	306
UiO-66-NH_2-25	1284	1378	295
UiO-66-NH_2-50	1252	1361	288
UiO-66-NH_2-75	1198	1298	275
UiO-66-NH_2	1161	1254	267

3.4 Chemical stability

The chemical stability of the series of materials was confirmed by measuring PXRD patterns before and after the treatment with aqueous (at RT and 100 °C), acidic (1M HCl), and basic (1M NaOH) media. Figure 7 shows the results of chemical stability tests on UiO-66, UiO-66-NH_2-50 and UiO-66-NH_2 (see Figure S10 for the results on UiO-66-NH_2-25 and UiO-66-NH_2-75). The PXRD pattern obtained of the samples after the aqueous treatments (RT for 2 months and under

reflux for 24 hours) do not show any significant change. However porosity of these samples when refluxed in water for 24h show significant decrease in the porosity (Figure S11). Interestingly, ABDC functionalized MOFs were found to degrade more slowly than UiO-66 under acidic conditions, as previously reported by Krista and coworkers.[40] Of course all samples undergo complete amorphization under basic conditions.

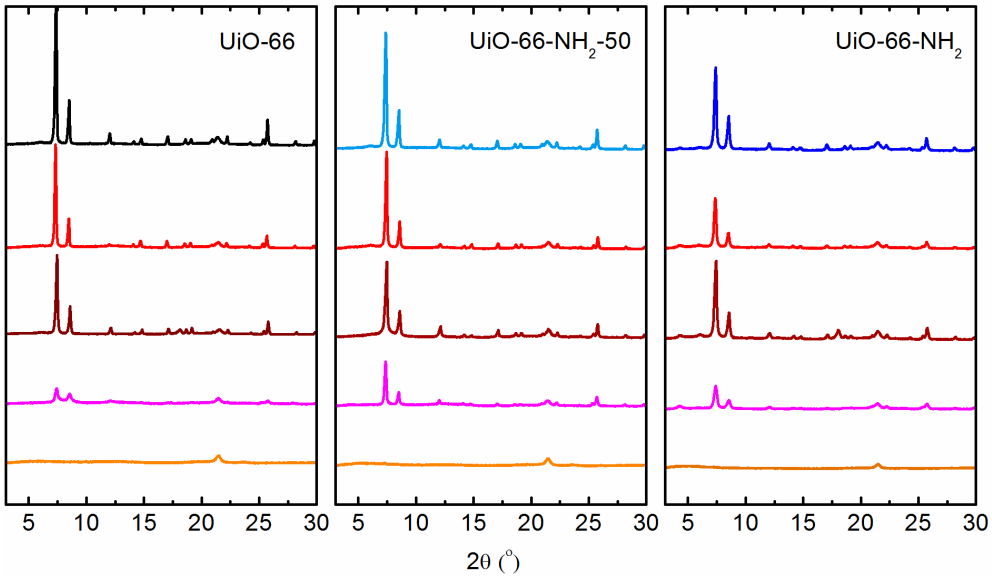

Figure 7. Powder XRD patterns of MOFs as prepared (with same color code used in previous figures), and after the treatment of 1 month in water(red), 24h reflux in water (brown),24h in 1M HCl (magenta) and 24h 1M NaOH (orange).

4. Conclusion

A series of mixed linker–MOFs with UiO-66 topology have been successfully prepared using mixture of ABDC and BDC. The thermal stability and porosity of the frameworks are significantly influenced by the ratio between ABDC and BDC in the framework. With this series we have successfully demonstrated, that UV-Vis spectroscopy can be used for the quantitative determination of ABDC in mixed-linker–MOFs. We have also demonstrated that 1M NaOH can be used as a media for the disassembly of Zr-based MOFs for the quantitative analysis of linkers in amine functionalized mixed-linker–MOFs. By providing a method which allows control over the loading of the amino functionality, many opportunities for further studies on sorption and post synthetic modifications are afforded.

Acknowledgement

The Research Council of Norway (CLMIT project no. 215735), VISTA (project no. 6457) and MIUR-PRIN 2010-2011(project n: 2010A2FSS9) are kindly acknowledged for the financial support. We thank Sharmala Aravinthan for her help in material synthesis and characterization.

Supporting information

Synthetic details, methods of quantitative analysis of ABDC by UV-visible and ^{1}HNMR spectroscopy, key results for materials prepared with modified reaction conditions, TG-DSC comparison of physical mixture and UiO-66-NH_2-50, and thermal treatments followed by PXRD. This material is available free of charge via the internet at http://pubs.acs.org.

References

1. Eddaoudi, M.; Moler, D. B.; Li, H. L.; Chen, B. L.; Reineke, T. M.; O'Keeffe, M.; Yaghi, O. M., *Accounts Chem. Res.* **2001,** *34* (4), 319.

2. Yaghi, O. M.; O'Keeffe, M.; Ockwig, N. W.; Chae, H. K.; Eddaoudi, M.; Kim, J., *Nature* **2003,** *423* (6941), 705.

3. Kitagawa, S.; Kitaura, R.; Noro, S., *Angew. Chem.-Int. Edit.* **2004,** *43* (18), 2334.

4. Ferey, G., *Chemical Society Reviews* **2008,** *37* (1), 191.

5. Morris, R. E.; Wheatley, P. S., *Angew. Chem.-Int. Edit.* **2008,** *47* (27), 4966.

6. Li, J. R.; Sculley, J.; Zhou, H. C., *Chem. Rev.* **2012,** *112* (2), 869.

7. Farrusseng, D.; Aguado, S.; Pinel, C., *Angew. Chem.-Int. Edit.* **2009,** *48* (41), 7502.

8. Lee, J.; Farha, O. K.; Roberts, J.; Scheidt, K. A.; Nguyen, S. T.; Hupp, J. T., *Chem. Soc. Rev.* **2009,** *38* (5), 1450.

9. Corma, A.; Garcıa, H.; Llabres i Xamena, F. X., *Chem. Rev.* **2010,** *110* (8), 4606.

10. Cunha, D.; Ben Yahia, M.; Hall, S.; Miller, S. R.; Chevreau, H.; Elkaim, E.; Maurin, G.; Horcajada, P.; Serre, C., *Chem. Mater.* **2013,** *25* (14), 2767.

11. Cunha, D.; Gaudin, C.; Colinet, I.; Horcajada, P.; Maurin, G.; Serre, C., *J. Mater. Chem. B* **2013,** *1* (8), 1101.

12. Wang, Z.; Tanabe, K. K.; Cohen, S. M., *Inorg. Chem.* **2008,** *48* (1), 296.

13. Cohen, S. M., *Chem. Rev.* **2011,** *112* (2), 970.

14. Gascon, J.; Aktay, U.; Hernandez-Alonso, M. D.; van Klink, G. P. M.; Kapteijn, F., *J. Catal.* **2009,** *261* (1), 75.

15. Kandiah, M.; Nilsen, M. H.; Usseglio, S.; Jakobsen, S.; Olsbye, U.; Tilset, M.; Larabi, C.; Quadrelli, E. A.; Bonino, F.; Lillerud, K. P., *Chem. Mater.* **2010,** *22* (24), 6632.

16. Vermoortele, F.; Ameloot, R.; Vimont, A.; Serre, C.; De, V. D., *Chem. Commun.* **2011,** *47* (5), 1521.

17. Roy, P.; Schaate, A.; Behrens, P.; Godt, A., *Chem. - Eur. J.* **2012,** *18* (22), 6979.

18. Yang, Q. Y.; Wiersum, A. D.; Llewellyn, P. L.; Guillerm, V.; Serred, C.; Maurin, G., *Chem. Commun.* **2011,** *47* (34), 9603.

19. Cmarik, G. E.; Kim, M.; Cohen, S. M.; Walton, K. S., *Langmuir* **2012,** *28* (44), 15606.

20. Sumida, K.; Rogow, D. L.; Mason, J. A.; McDonald, T. M.; Bloch, E. D.; Herm, Z. R.; Bae, T. H.; Long, J. R., *Chem. Rev.* **2012,** *112* (2), 724.

21. Farha, O. K.; Hupp, J. T., *Accounts Chem. Res.* **2010,** *43* (8), 1166.

22. Burrows, A. D., *CrystEngComm* **2011,** *13* (11), 3623.

23. Das, M. C.; Xiang, S. C.; Zhang, Z. J.; Chen, B. L., *Angew. Chem.-Int. Edit.* **2011,** *50* (45), 10510.

24. Bunck, D. N.; Dichtel, W. R., *Chem. - Eur. J.* **2013,** *19* (3), 818.

25. Foo, M. L.; Matsuda, R.; Kitagawa, S., *Chem. Mater.* **2013,** *26* (1), 310.

26. Kleist, W.; Maciejewski, M.; Baiker, A., *Thermochim. Acta* **2010,** *499* (1-2), 71.

27. Marx, S.; Kleist, W.; Huang, J.; Maciejewski, M.; Baiker, A., *Dalton Trans.* **2010,** *39* (16), 3795.

28. Lescouet, T.; Kockrick, E.; Bergeret, G.; Pera-Titus, M.; Aguado, S.; Farrusseng, D., *J. Mater. Chem.* **2012,** *22* (20), 10287.

29. Reinsch, H.; Waitschat, S.; Stock, N., *Dalton Trans.* **2013,** *42* (14), 4840.

30. Lammert, M.; Bernt, S.; Vermoortele, F.; De Vos, D. E.; Stock, N., *Inorg. Chem.* **2013,** *52* (15), 8521.

31. Cavka, J. H.; Jakobsen, S.; Olsbye, U.; Guillou, N.; Lamberti, C.; Bordiga, S.; Lillerud, K. P., *J. Am. Chem. Soc.* **2008,** *130* (42), 13850.

32. Valenzano, L.; Civalleri, B.; Chavan, S.; Bordiga, S.; Nilsen, M. H.; Jakobsen, S.; Lillerud, K. P.; Lamberti, C., *Chem. Mater.* **2011,** *23* (7), 1700.

33. Kim, M.; Cohen, S. M., *CrystEngComm* **2012,** *14* (12), 4096.

34. Chavan, S.; Vitillo, J. G.; Gianolio, D.; Zavorotynska, O.; Civalleri, B.; Jakobsen, S.; Nilsen, M. H.; Valenzano, L.; Lamberti, C.; Lillerud, K. P.; Bordiga, S., *Phys. Chem. Chem. Phys.* **2012,** *14* (5), 1614.

35. Wang, Z. Q.; Cohen, S. M., *Chem. Soc. Rev.* **2009,** *38* (5), 1315.

36. Kandiah, M.; Usseglio, S.; Svelle, S.; Olsbye, U.; Lillerud, K. P.; Tilset, M., *J. Mater. Chem.* **2010,** *20* (44), 9848.

37. Ranocchiari, M.; Lothschuetz, C.; Grolimund, D.; van Bokhoven, J. A., *Proc. R. Soc. A* **2012,** *468* (2143), 1985.

38. Kim, M.; Cahill, J. F.; Prather, K. A.; Cohen, S. M., *Chem. Commun.* **2011,** *47* (27), 7629.

39. Shearer, G. C.; Chavan, S. M.; Ethiraj, J.; Vitillo, J. G.; Svelle, S.; Olsbye, U.; Lamberti, C.; Bordiga, S.; Lillerud, K. P., *Chem. Mater.* **2014**.

40. DeCoste, J. B.; Peterson, G. W.; Jasuja, H.; Glover, T. G.; Huang, Y. G.; Walton, K. S., *J. Mater. Chem. A* **2013,** *1* (18), 5642.

TOC graphics

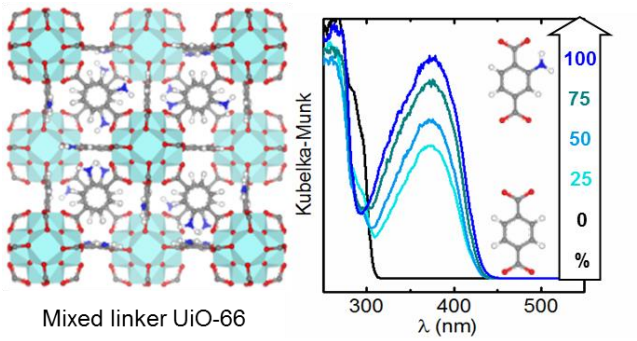

Table of content Synopsis

A series of amine functionalized mixed–linker MOFs of UiO-66 topology has been prepared and thoroughly characterized by TGA, PXRD, Uv-visible and FTIR spectroscopy with the aim of elucidating the effect that varying degrees of amine functionalisation has on the stability (thermal and chemical) and porosity of the framework. This work includes the first application of UV-visible spectroscopy in the quantification of ABDC in mixed linker–MOFs.

Supporting information

Synthesis and Characterization of Amine Functionalized Mixed Ligand Metal-organic Frameworks of UiO-66 topology

Sachin M. Chavan[a*], Greig C. Shearer[a], Stian Svelle[a], Unni Olsbye[a], Francesca Bonino[b], Jayashree Ethiraj[b], Karl Petter Lillerud[a] and Silvia Bordiga[a, b*]

[a]*inGAP Center of Research Based Innovation, Department of Chemistry, University of Oslo, P.O. Box 1033, Blindern, 0315 Oslo, Norway*

[b]*Department of Chemistry, NIS and INSTM Reference Centre, University of Turin, Via G. Quarello 15 I-10135 Torino, Italy*

Table of Content

Sections	Content	page
A	Synthesis details and powder X-ray diffractions patterns (3-50^{o}) of the mixed linker -MOFs prepared at 100 $^{\circ}$C with M:L ration 1:1 and without addition of HCl.	3
B	Diffuse Reflectance UV-visible spectra of mixed linker -MOF series washed with DMF.	4
C	UV-visible absorbance Spectra of ABDC standard solutions in 1M NaOH	4
D	PXRD and TGA-DSC of the undissolved solid obtained after MOF digestion.	5
E	Quantitative analysis of ABDC linker in the mixed linker -MOFs series by UV-visible spectroscopy.	6
F	Quantitative analysis of ABDC linker in the mixed linker-MOFs series by ^{1}H-NMR spectroscopy	7-9
G	Synthesis, PXRD, ^{1}H NMR spectra and N_2 sorption of mixed linker -MOFs series prepared at 220 $^{\circ}$C with M:L=1:2, 2 molar equivalents of HCl	10
H	Comparison of TG-DSC results of UiO-66-NH_2-50 with a 1:1 physical mixture of UiO-66 + UiO-66-NH_2	11
I	Thermal stability of mixed linker–MOFs: PXRD	12
J	PXRD after N_2 sorption experiments	13
K	Chemical stability plots for UiO-66-NH_2-25 and UiO-66-NH_2-75	13
L	N_2 adsorption on MOFs refluxed in water for 24h.	14

A) Synthesis details and powder X-ray diffractions patterns (3-50°) of the mixed linker –MOFs prepared at 100 °C with M:L ration 1:1 and without addition of HCl.

Table S1. Synthesis of the Mixed ligand MOFs

MOFs	Reagent amount				
	$ZrCl_4$ (g)	BDC (g)	ABDC (g)	H_2O (ml)	DMF (ml)
UiO-66	1	0.712	0	0.10	110
UiO-66-NH_2-25	1	0.5346	0.1943	0.10	110
UiO-66-NH_2-50	1	0.3564	0.3886	0.10	110
UiO-66-NH_2-75	1	0.1782	0.5830	0.10	110
UiO-66-NH_2	1	0	0.7773	0.10	110

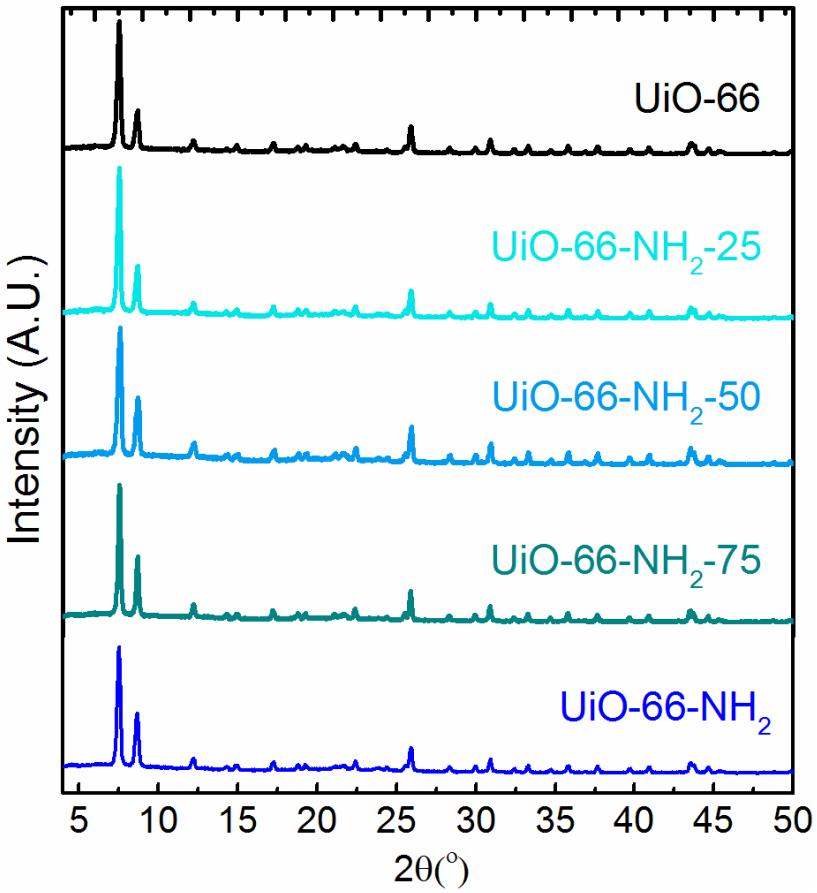

Figure S1: Comparison of the powder X-ray diffraction patterns of the as synthesized mixed linker –MOF series in the 4-50°, 2θ range.

B) Diffuse Reflectance UV-visible spectra of as synthesized mixed linker–MOFs series.

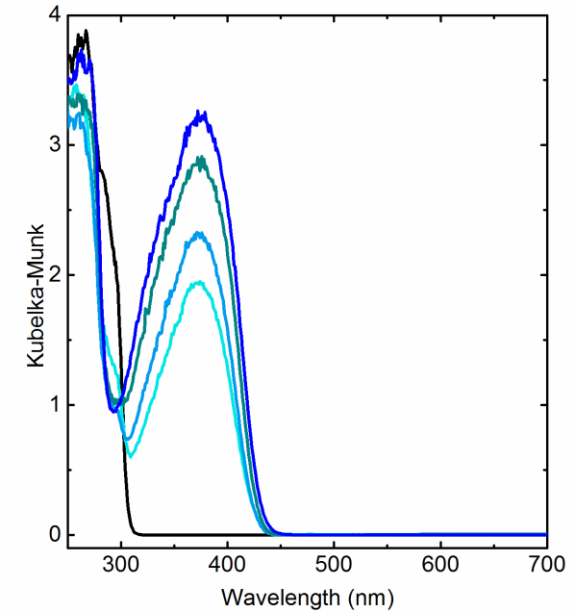

Figure S2. Diffuse reflectance Uv-visible spectra of samples containing DMF: UiO-66, UiO-66-NH_2-25, UiO-66-NH_2-50, UiO-66-NH_2-75, and UiO-66-NH_2.

C) UV-visible absorbance spectra of ABDC standard solution in 1M NaOH .

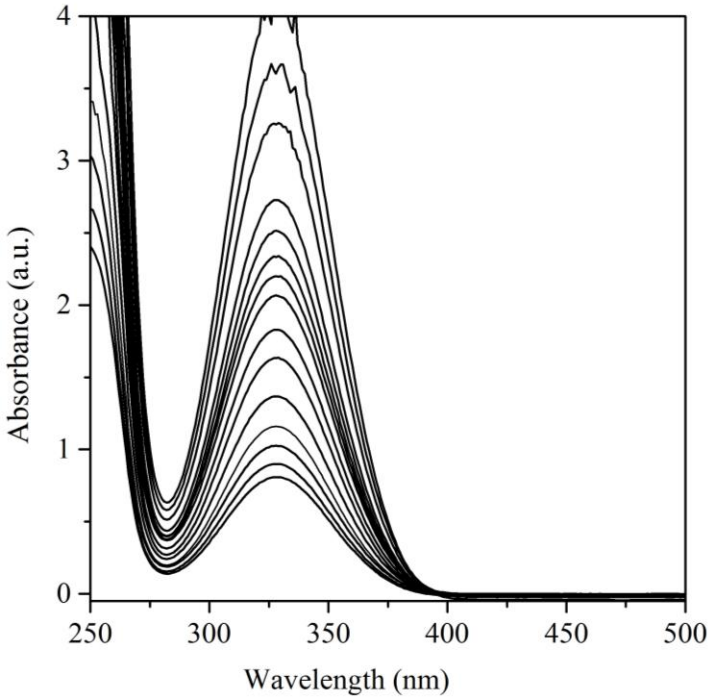

Figure S3: Absorbance spectra of the ABDC standard solutions in 1M aqueous NaOH solution. These spectra are used to obtain the calibration curve shown in figure 2 inset of the paper.

D) PXRD and TGA-DSC of the undissolved solid obtained after MOF digestion.

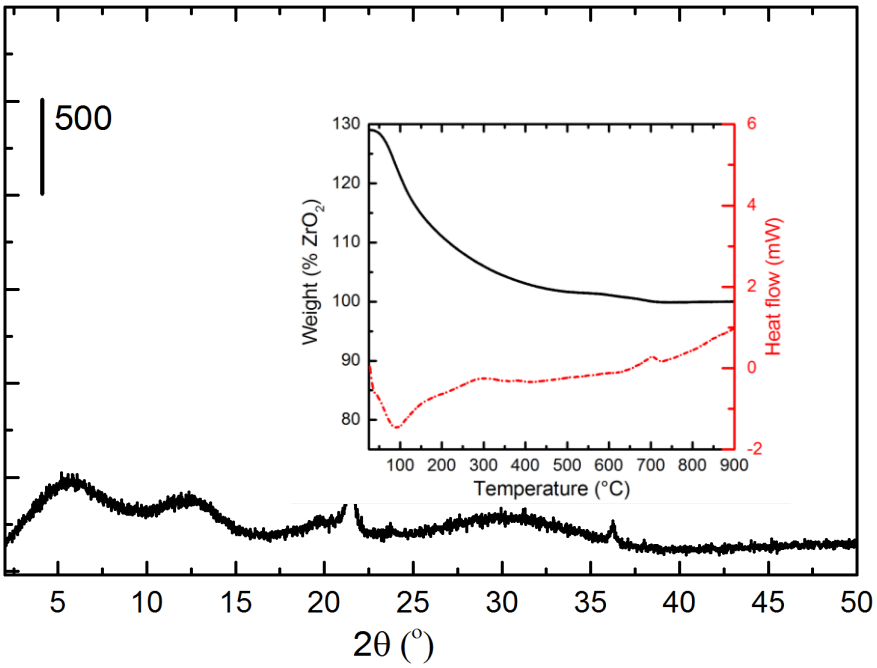

Figure S4. The PXRD and TG-DSC of the undissolved solid obtained after the digestion of UiO-66-NH_2 MOF sample in 1M NaOH. PXRD clearly shows no sign of residual MOF while TG-DSC results show no weight loss and exothermic heat signal expected for the burning of ligand/organic residue. In the diffraction pattern a peak at 21.41, 2θ is due to the plastic foil used to cover the sample while collecting the data.

E) Quantitative analysis of ABDC linker in the mixed linker-MOFs series by UV-visible spectroscopy.

Table S2. The quantitative analyses of ABDC linker in the series of mixed linker-MOFs, Samples were digested in 35 ml of 1M NaOH-D_2O for 24h. Absorbance spectra of solutions were recorded after filtering out the white precipitate (most probably of zirconium hydroxide).

MOF	Sample Mass mg	Actual mass of MOF[a] mg	Calc. mass of ABDC[b] mg	Calc. [ABDC×10^{-4}][c] mol L^{-1}	Exp. [ABDC×10^{-4}] mol L^{-1}	Exp. mol % of ABDC [d]
UiO-66-NH_2	10.1	7.07	4.34	6.42	6.69	104
UiO-66-NH_2-75	10.4	7.28	3.39	5.02	4.70	70
UiO-66-NH_2-50	15.5	10.85	3.41	5.06	5.50	54
UiO-66-NH_2-25	20.0	14.0	2.23	3.31	4.0	30

[a]Actual mass of MOF (65 weight % of the sample Mass) is the sample mass excluding solvent.

[b]Theoretical mass of ABDC = $\frac{6X \cdot M.W.of\ ABDC}{Theo.\ M.W.of\ MOF} \times Actual\ mass\ of\ MOF$, where x and the theoretical molecular weight of MOF is derived from the idealized chemical formula: $Zr_6(O)_4(OH)_4(ABDC)_{6x}(BDC)_{6-6x}$, where x = 0.25, 0.5, 0.75, and 1, for UiO-66-NH_2-25, -50, -75, and UiO-66-NH_2 respectively.

[c] Theoretical $[ABDC] = \frac{Theo.\ Mass\ of\ ABDC}{M.W.\ of\ ABDC \cdot 35 \cdot 10^{-3}\ L}$

[d] mol% of ABDC $= \frac{Experimental[ABDC]}{Theoretical[ABDC]} \cdot x \cdot 100\ \%$

F) Quantitative analysis of ABDC linker in the mixed linker-MOFs series by ^{1}H-NMR spectroscopy

The mol % of ABDC was calculated from the integrals by first integrating the BDC signal (Figure 3a) and defining the integral as 12 protons (3 molecules, since the number of protons represented by the BDC signal is 4). The 3 ABDC signals were then integrated relative to this number (Figure 3b). In order for the relative concentration of ABDC to be represented by one number, the average of the three integrals (representing 1 proton each) was used. Finally, the following three formulae were applied to calculate the ABDC content of the samples:

$$No.BDC\ molecules = \frac{BDC\ integral}{No.\ H\ Rep.(=4)}$$

$$Relative\ No.ABDC\ molecules = \frac{Mean\ ABDC\ integral}{No.\ H\ Rep\ (=1)}$$

$$mol\%.ABDC = \frac{Rel.No.ABDC\ molecule}{No.BDC\ molecule + Rel.No.ABDC\ molecule}$$

G) Synthesis, PXRD and ^{1}HNMR spectra of mixed linker–MOFs series prepared with M:L=1:2, and 2 molar equivalent of HCl at 220 °C.

Table S3. Synthesis of Mixed linker-MOFs prepared at 220 °C

MOFs	Reagent amount				
	$ZrCl_4$ (g)	BDC (g)	ABDC (g)	HCL (ml)	DMF (ml)
UiO-66	3.52	5.02	0	2.68	91.25
ML-MOF-1	3.52	3.77	1.37	2.68	91.25
ML-MOF-2	3.52	2.51	2.73	2.68	91.25
ML-MOF-3	3.52	1.25	4.10	2.68	91.25
UiO-66-NH_2	3.52	0	5.64	2.68	91.25

In this series of samples, the total amount of DMF was split in two/three equal parts for the synthesis of phase pure/mixed linker–MOFs respectively. $ZrCl_4$, BDC and ABDC were dissolved separately in different portions of DMF. All 35% HCl was added to the flask designated to $ZrCl_4$ prior to the addition of metal salt. Following the successful dissolution of all synthesis components, the two/three solutions were mixed together, transferred to 200 ml Teflon-lined autoclaves, and heated to 220 °C for 20 hours under static conditions. The powder precipitates were filtered, washed in boiling water and finally dried at 60 °C in air.

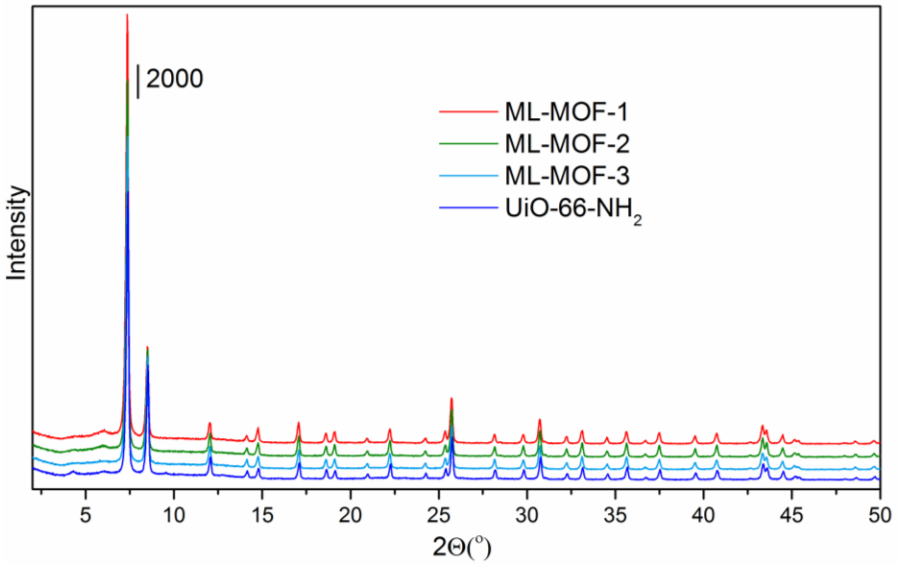

Figure S4. Comparison of the PXRD patterns of the mixed linker-MOFs.

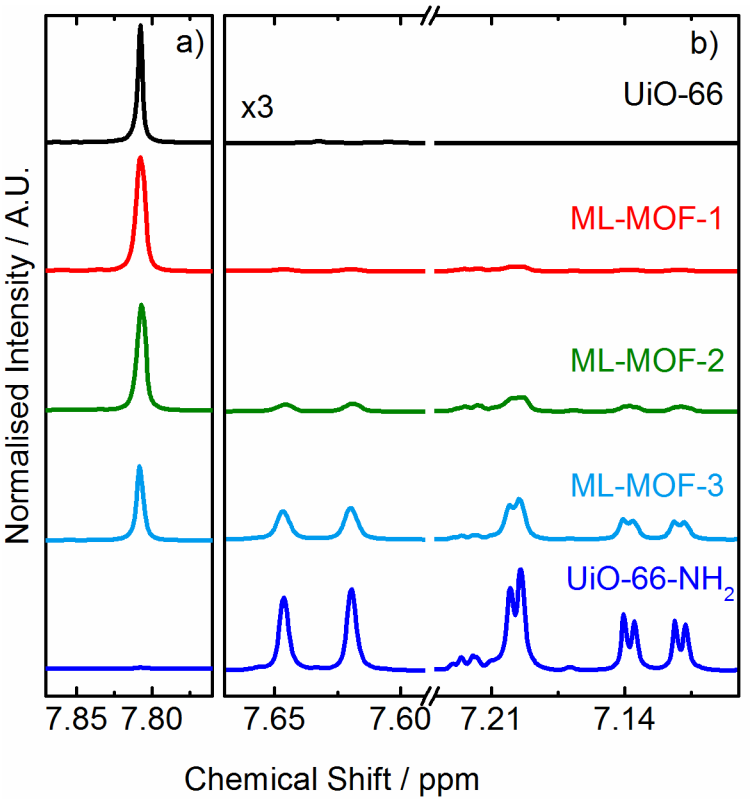

Figure S5. Normalized ^{1}H NMR spectra of digested samples of a mixed linker–MOF series prepared at 220 $^{\circ}$C and with a metal to linker ratio of 1:2. Samples were digested for 24h in a 1M solution of NaOH in D_2O. Signals of ABDC proton in part b are multiplied by factor of 3, for easy visual comparison of the signal intensities.

Table S4. mol% of ABDC determined by ^{1}HNMR spectroscopy.

Sample	mol % of ABDC
ML-MOF-1	4
ML-MOF-2	15
ML-MOF-3	53
UiO-66-NH_2	100

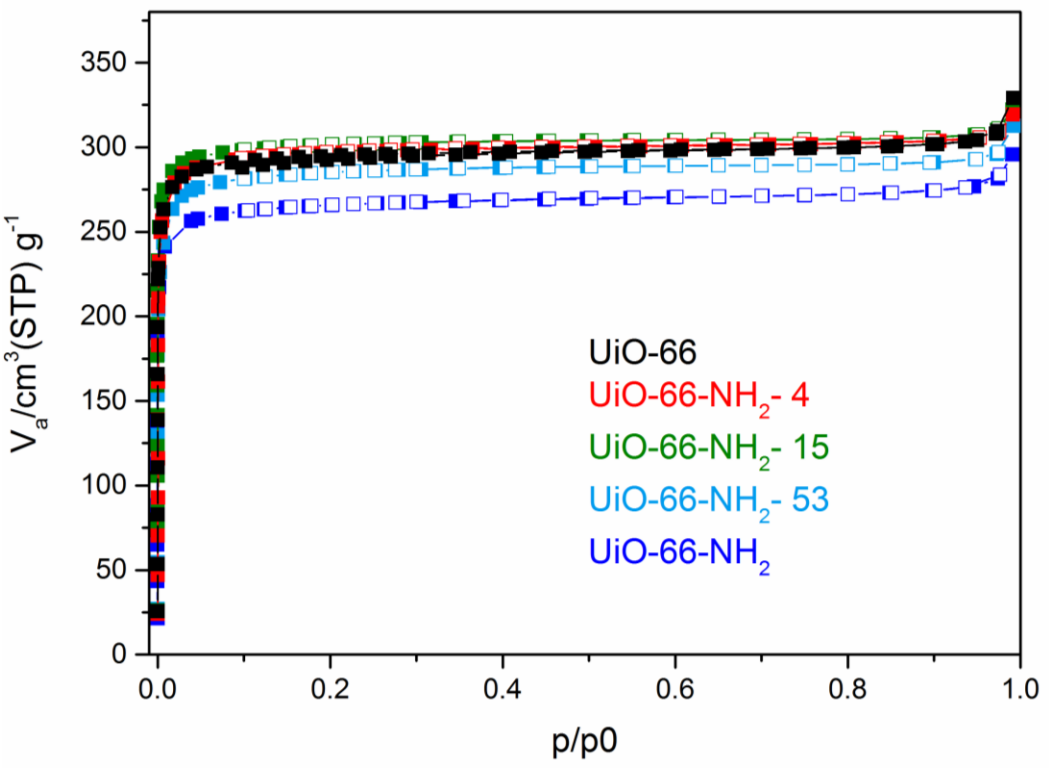

Figure S6. N_2 adsorption at 77K on the set of mixed linker-MOF prepared at 220 °C with 1:2 metal to linker ration, and with addition of HCl.

H) Comparison of TG-DTA results of UiO-66-NH_2-50 with 1:1 physical mixture of UiO-66 + UiO-66-NH_2.

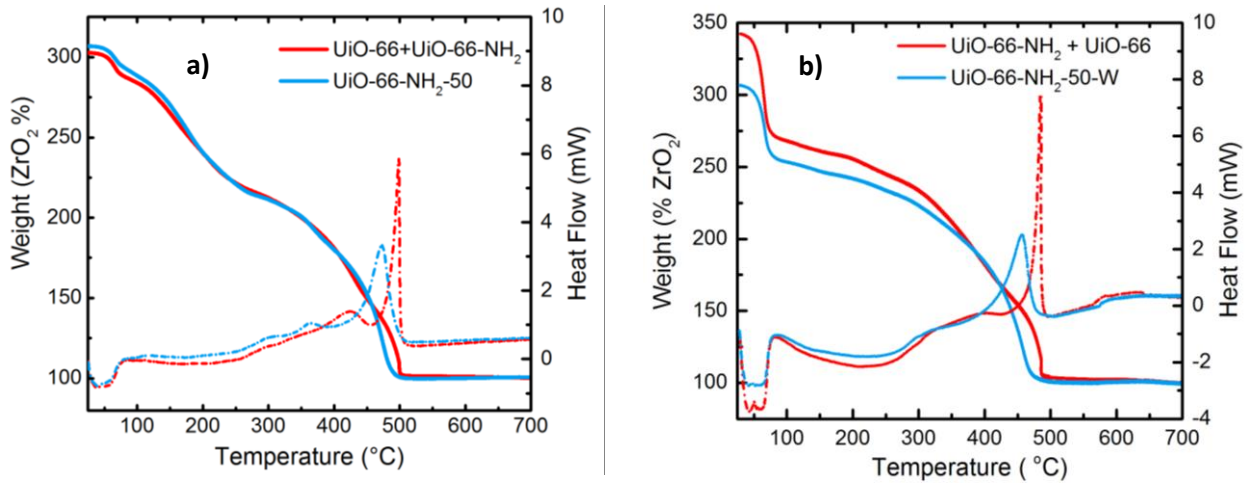

Figure S7. TGA-DSC analyses of physically prepared mixture with 1:1 molar ration of UiO-66 and UiO-66-NH_2, with UiO-66-NH_2 -50. Part A and B show the data obtained on as prepared and water washed samples respectively. Samples were heated from 25 to700 $^{\circ}$C, at rate of 1 $^{\circ}$C min^{-1} under dry air flux (N_2, at 20ml/min and O_2 at, 5ml/min).

As previously seen, very little difference in the weight loss behavior and the distinct, broad heat signal for UiO-66-NH_2-50 is observed for water washed samples. This not only confirms the reproducibility of the data but also prove our proposed hypothesis that the sample prepared here indeed contain randomly distributed linker and not the mixture of separate phase.

I) Thermal stability of mixed linker –MOFs :PXRD

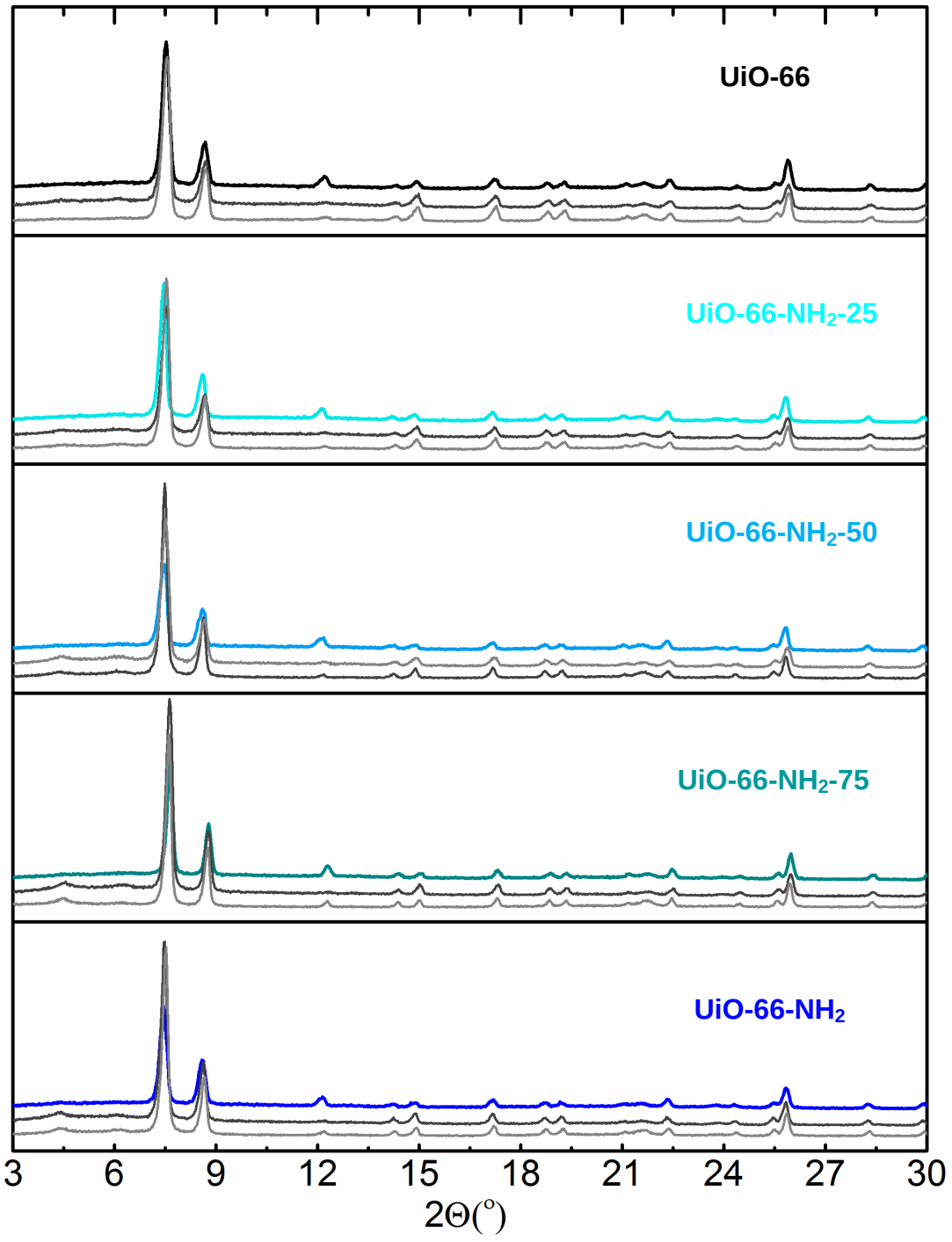

Figure S8: Powder XRD patterns of a) UiO-66, b) UiO-66-NH_2-25, c) UiO-66-NH_2-50, d) UiO-66-NH_2-75 and e) UiO-66-NH_2. Within each plot are three curves which from top to bottom represent the sample as synthesized (with the same color code used in previous figures), water washed (dark grey) and after heating at 200 °C for 12h in air (grey).

J) PXRD after N_2 sorption experiments

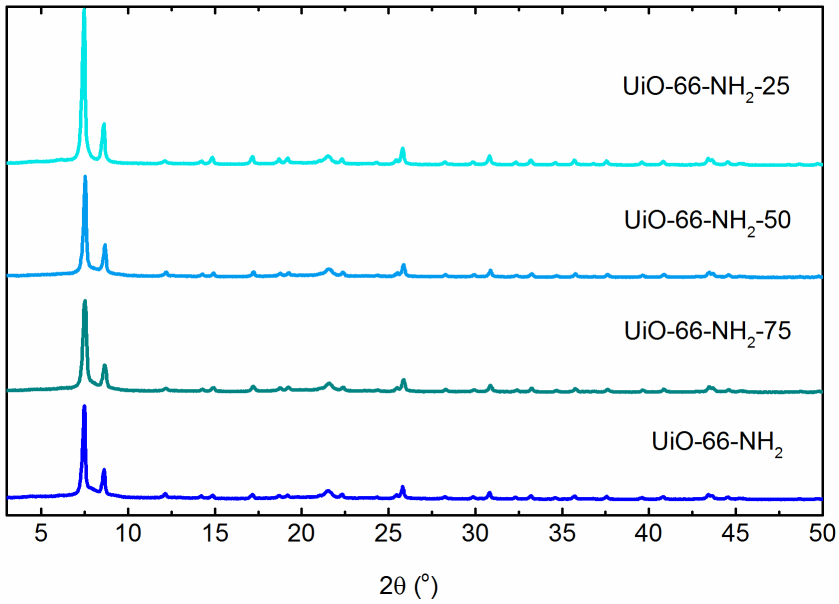

Figure S9: PXRD patterns of the mixed linker -MOFs after N_2 sorption experiments, elucidating the framework stability to the removal of solvents.

K) Chemical stability of UiO-66-NH_2-25 and UiO-66-NH_2-75.

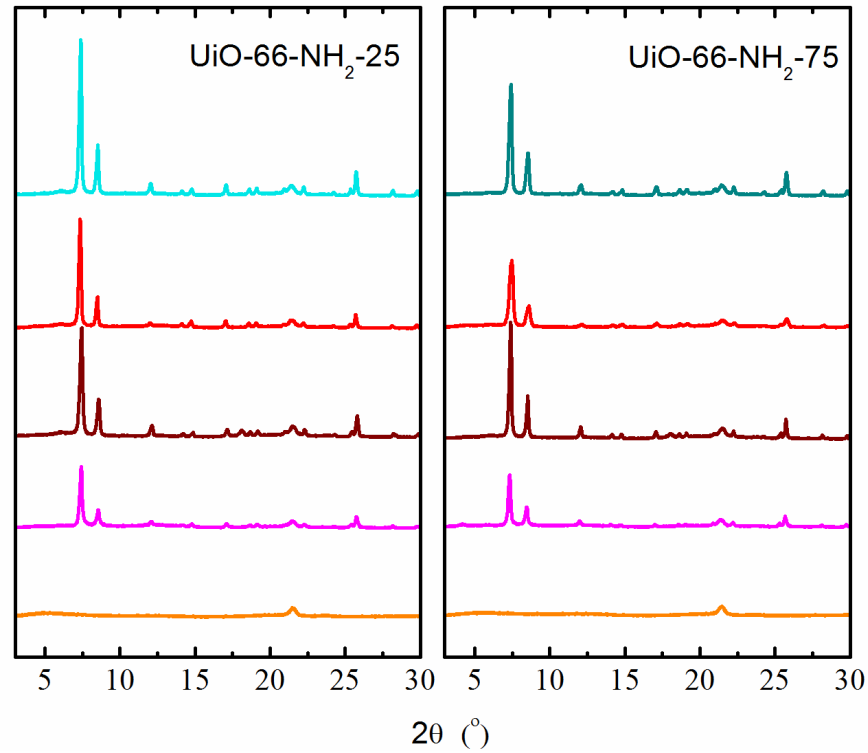

Figure S10: PXRD patterns of MOFs as prepared (with same color code used in previous figures), and after the treatment of 1 month in water(red), 24h reflux in water (brown),24h in 1M HCl (magenta) and 24h 1M NaOH (orange).

L) **N_2 adsorption on MOFs refluxed in water for 24h**.

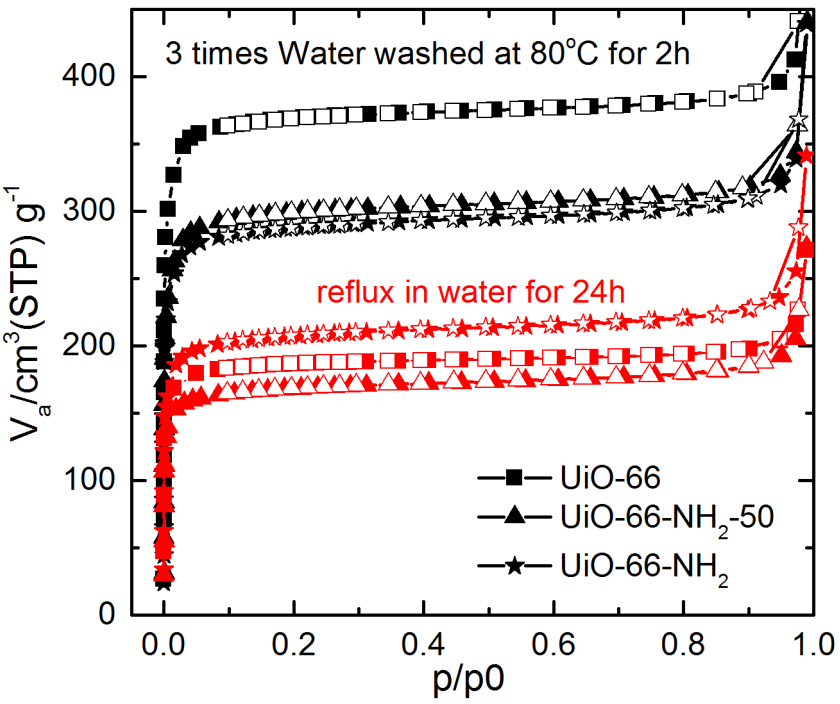

Figure S11. N_2 sorption of MOFs; UiO-66 (square), UiO-66-NH2-50 (triangle) and UiO-66-NH_2 (star) water washed at 80 °C (black) and after reflux in water for 24h (red).